Kondo lattice behavior and magnetic ordering in $CeRh_2Si$

D. Kaczorowski[1] and A. Ślebarski[2]
[1]*Institute of Low Temperature and Structure Research, Polish Academy of Sciences, P.O. Box 1410, 50-950 Wrocław, Poland*
[2]*Institute of Physics, University of Silesia, 40-007 Katowice, Poland*
(Received 19 April 2010; revised manuscript received 14 May 2010; published 9 June 2010)

Polycrystalline samples of $CeRh_2Si$ were studied by means of magnetic, electrical transport, heat capacity, and x-ray photoemission measurements. The compound was found to order magnetically at 1.65 K at odds with the literature data. The behavior of the resistivity and the specific heat in applied magnetic field suggests an antiferromagnetic character of the electronic ground state. The electrical resistivity varies with temperature in a manner typical for dense Kondo systems with distinct crystal-field interactions. The Kondo effect manifests itself also in enhanced electronic contribution to the specific heat, reduced specific-heat jump at the onset of the ordered state, and strongly reduced entropy released by the magnetic phase transition. The characteristic energy scale in $CeRh_2Si$, derived from the magnetic and heat-capacity data, is 12–16 K. The Kondo interactions lead to some valence instability of the cerium $4f$ shell that was inferred from the core level $3d$ and $4d$ x-ray photoelectron spectra of the compound studied.

DOI: 10.1103/PhysRevB.81.214411 PACS number(s): 75.30.Mb, 72.15.Qm, 75.50.Ee, 71.27.+a

I. INTRODUCTION

Recent discoveries of unconventional superconductivity in noncentrosymmetric heavy-fermion compounds $CePt_3Si$,[1] $CeRhSi_3$,[2] and $CeIrSi_3$ (Ref. 3) revived much interest in investigating cerium silicides containing noble metals. In the ternary system Ce-Rh-Si, the existence of as many as 25 ternary compounds has been reported.[4] The most studied material until now has been $CeRh_2Si_2$ that exhibits at low temperatures strongly anisotropic antiferromagnetic ordering,[5] which is replaced under hydrostatic pressure by a superconducting state.[6] Most spectacularly, both cooperative phenomena coexist in some pressure range around the critical value of 0.9 GPa.[6,7] Similarly, the superconductivity in $CeRhSi_3$ evolves from the antiferromagnetic ground state near the quantum critical point at $p_c=2.4$ GPa.[2] The uniqueness of superconductivity in $CeRhSi_3$, as well as in $CePt_3Si$,[1] $CeIrSi_3$,[3] and probably UIr (Ref. 8) comes from the fact that it involves spin fluctuations—assisted triplet pairing, which has hitherto been believed to be feasible only in compounds possessing centrosymmetric crystal structures.[9] Other ternaries from the system Ce-Rh-Si span wide spectrum of physical properties from valence fluctuations [e.g., $CeRhSi_2$ and $Ce_2Rh_3Si_5$ (Ref. 10)] via antiferromagnetic Kondo lattice behavior [e.g., Ce_2RhSi_3 (Ref. 11)] to complex long-range magnetic orderings [e.g., $Ce_3Rh_3Si_2$ (Ref. 12) and $CeRh_3Si_2$ (Ref. 13)].

Formation of the compound $CeRh_2Si$ was first communicated by Tursina *et al.*,[14] who determined the crystal structure of this phase to be a site exchange variant of the orthorhombic $CeNiSi_2$ type. The physical behavior of the new silicide was studied by Muro *et al.*[15] The authors described the compound as a heavy-fermion system, which shows a spin-glass transition at 1 K. In this paper we report on the results of our independent investigation of $CeRh_2Si$ aimed mainly at ascertaining its low-temperature (LT) behavior.

II. EXPERIMENTAL DETAILS

Polycrystalline sample of $CeRh_2Si$ was prepared by arc-melting stoichiometric amounts of the constituents (Ce: Ames Laboratory, 99.9 mass %; Rh: Chempur, 99.9 mass %; and Si: Chempur, 6N) under titanium-gettered argon atmosphere. The button was turned over and remelted several times to ensure good homogeneity. Subsequently, it was wrapped with tantalum foil and annealed at 850 °C for 5 weeks.

Quality of the annealed sample was checked by means of x-ray diffraction (Stoe powder diffractometer with Cu $K\alpha$ radiation) and microprobe analysis [Phillips 515 scanning electron microscope equipped with an energy-dispersive x-ray analysis (EDAX) PV 9800 spectrometer]. The lattice parameters derived from the x-ray data amount to $a=4.0448(8)$ Å, $b=17.750(4)$ Å, and $c=4.058(1)$ Å, being in good agreement with the literature values.[14] Moreover, the intensities of the x-ray reflections are consistent with the atom arrangement within the $CeNiSi_2$-type related unit cell given in Ref. 16. Besides the peaks due to the major phase two weak foreign reflections were observed on the diffraction pattern, which marked the presence of small amount (less than 5%) of $CeRh_3Si_2$ as an impurity. The EDAX yielded the composition 24.3(8):49.1(4):26.7(9) of the main phase, in fairly good agreement with the nominal one. Moreover, it corroborated some contamination of the sample studied by $CeRh_3Si_2$. It is worth to mention that very similar metallurgical problem in obtaining single-phase material was reported for $CeRh_2Si$ in Ref. 15.

Magnetic measurements were performed in the temperature range 1.72–400 K and in magnetic fields up to 5 T using a Quantum Design MPMS-5 superconducting quantum interference device magnetometer. The heat capacity and the electrical resistivity were measured over the interval 0.35–10 K and 0.35–300 K, respectively, employing a Quantum Design PPMS-9 platform. For the transport studies the current and voltage leads were attached to a parallelepiped-shaped specimen by tin soldering and spot welding, respectively. The transverse ($i \perp B$) magnetoresistance was measured in magnetic fields up to 9 T within the temperature range 0.35–30 K. Independently, the transverse magnetoresistivity was measured in the temperature interval 4.2–60 K in fields up to 8 T using a homemade setup.

 ©2010 The American Physical Society

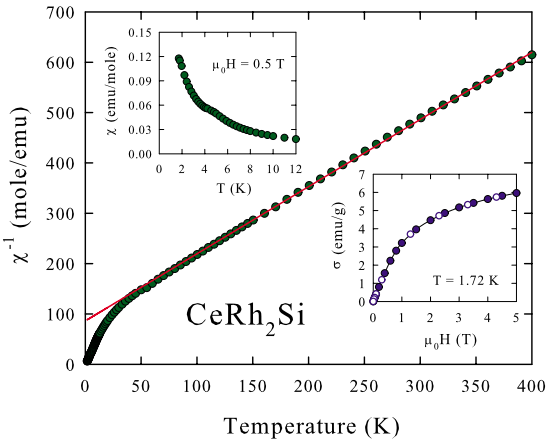

FIG. 1. (Color online) Temperature variation in the reciprocal molar magnetic susceptibility of $CeRh_2Si$ measured in a field of 0.5 T. The solid line is a Curie-Weiss fit with the parameters given in the text. Upper inset: low-temperature magnetic susceptibility of $CeRh_2Si$. Lower inset: field variation in the magnetization in $CeRh_2Si$ taken at $T=1.72$ K with increasing (full circles) and decreasing (open circles) magnetic field.

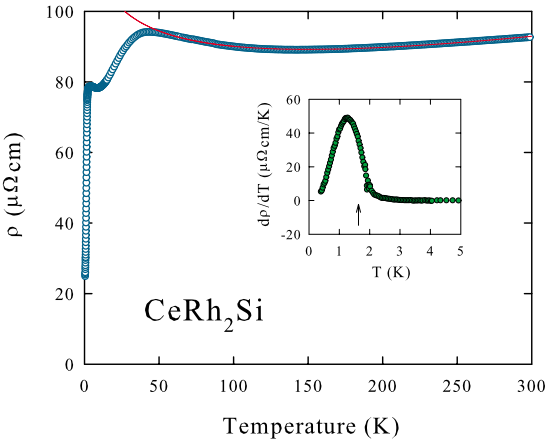

FIG. 2. (Color online) Temperature variation in the electrical resistivity of $CeRh_2Si$. The solid line is the Kondo fit discussed in the text. Inset: temperature dependence of the temperature derivative of the resistivity. The arrow denotes the magnetic phase transition observed in the specific-heat data.

X-ray photoelectron spectroscopy (XPS) experiments were carried out at room temperature using a Physical Electronics PHI 5700/660 spectrometer with monochromatized Al $K\alpha$ radiation (1486.6 eV). The spectra were collected on parallelepiped-shaped specimens broken *in situ* in high vacuum on the order of 10^{-10} Torr.

III. RESULTS AND DISCUSSION

A. Bulk physical properties

1. Magnetic susceptibility

The magnetic behavior of $CeRh_2Si$ is presented in Fig. 1. Above about 100 K the magnetic susceptibility follows a Curie-Weiss law with the effective magnetic moment $\mu_{\rm eff}=2.45\ \mu_B$ and the paramagnetic Weiss temperature $\theta_p=-65$ K. The value of $\mu_{\rm eff}$ is close to that expected for a Ce^{3+} ion within a Russell-Saunders coupling scheme, whereas the strongly negative θ_p value hints at the presence of Kondo interactions with a characteristic energy scale of about 16 K (Kondo temperature $T_K \simeq \theta_p/4$, Ref. 17). At lower temperatures, the inverse magnetic susceptibility considerably deviates from a straight-line behavior, presumably because of gradual depopulation of crystal-field levels originating from a cerium $^2F_{5/2}$ ground multiplet split in an orthorhombic crystal-field potential. As shown in the upper inset of Fig. 1, no indication of any magnetic ordering is observed down to 1.72 K, the lowest temperature achievable in the magnetic measurements performed (the small feature near 4.5 K should be attributed to small amount of $CeRh_3Si_2$,[13] detected as an impurity by the x-ray diffraction and in the EDX analysis). Indeed, at this terminal temperature the magnetization in $CeRh_2Si$ varies with magnetic field in a manner characteristic of paramagnetic ground state (see the lower inset of Fig. 1). The magnetization value reached in a field of 5 T corresponds to the magnetic moment of about 0.4 μ_B, which is only a very small fraction of the magnetic moment calculated for a free Ce^{3+} ion. The measured value is also significantly smaller than the moment that might be associated with a Kramers doublet being the crystal-field ground state upon lifting the degeneracy of the $^2F_{5/2}$ multiplet. This apparent strong reduction in the magnetic moment in $CeRh_2Si$ presumably arises due to Kondo screening effect.

2. Electrical transport

The Kondo interactions clearly manifest themselves in the temperature dependence of the electrical resistivity of $CeRh_2Si$, displayed in Fig. 2. The $\rho(T)$ curve is dominated by a maximum centered at about 40 K that is followed at higher temperatures by a negative slope, which can be described by the function

$$\rho(T) = \rho_0 + \rho_0^{\infty} + c_{\rm ph}T + c_K \ln T. \quad (1)$$

In this formula the terms ρ_0 and ρ_0^{∞} account for scattering conduction electrons on static lattice imperfections and disordered magnetic moments, respectively, the linear-in-T term is a simplified phonon contribution, whereas the logarithmic term represents spin-flip scattering on Kondo impurities. Fitting Eq. (1) to the experimental data yields the parameters: $(\rho_0+\rho_0^{\infty})_{\rm HT}=137.6\ \mu\Omega$ cm, $c_{\rm ph}=0.08\ \mu\Omega$ cm/K, and $c_{\rm K,HT}=-12.1\ \mu\Omega$ cm (HT means high-temperature region). The value of $c_{\rm K,HT}$ is similar to those observed for cerium-based Kondo lattices and hints at a considerable density of electronic states at the Fermi level. At low temperatures, the resistivity of $CeRh_2Si$ forms a shallow minimum near 10 K and then shows a rapid drop below 2 K. The value measured at 0.35 K is about 25 $\mu\Omega$ cm, yielding the residual resistivity ratio RRR=3.7.

The nonphononic resistivity $\Delta\rho$, derived by subtracting the phonon contribution $c_{\rm ph}T$ from the experimental data (it should be noted that such procedure may be inappropriate at low temperatures, where the assumption $c_{\rm ph}\sim T$ is likely incorrect, however in that region the contribution due to scat-

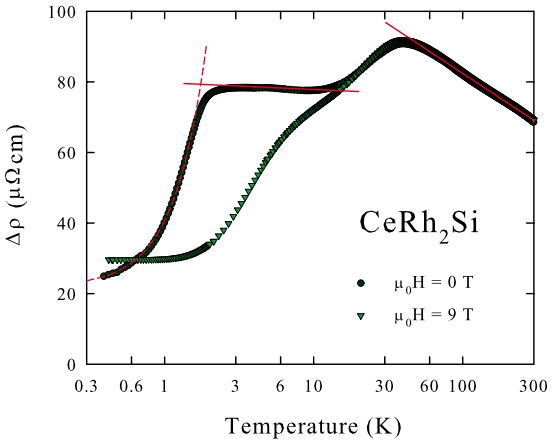

FIG. 3. (Color online) Temperature variation in the nonphononic electrical resistivity of $CeRh_2Si$ measured in zero magnetic field (circles) and in a field of 9 T applied perpendicular to the electrical current (triangles). Note the logarithmic temperature scale. The solid lines emphasize the LT and HT Kondo behavior. The dashed line is the low-temperature fit discussed in the text.

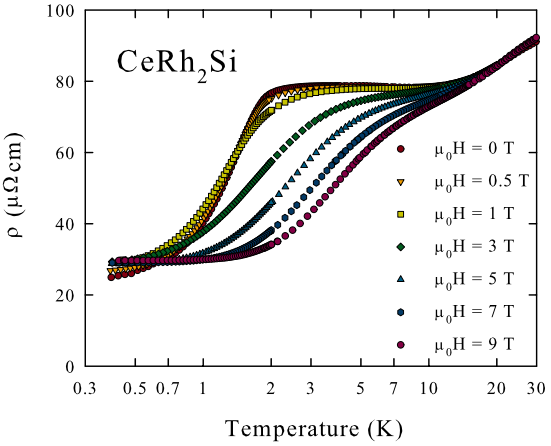

FIG. 4. (Color online) Low-temperature dependencies of the electrical resistivity of $CeRh_2Si$ measured in several different magnetic fields applied perpendicular to the electrical current. Note the logarithmic temperature scale.

tering of conduction electrons on phonons is anyway negligible in comparison to the other scattering mechanisms) is shown in Fig. 3. Clearly, besides the Kondo effect observed at high temperatures, another logarithmic slope in $\rho(T)$, yet of much smaller magnitude, is apparent at low temperatures, namely, below a resistivity minimum located at about 10 K. Analyzing the experimental data from the range 2.5–9 K (LT region) in terms of Eq. (1) gives the parameters: $(\rho_0+\rho_0^{\infty})_{\mathrm{LT}}=80.6\ \mu\Omega$ cm and $c_{\mathrm{K,HT}}=-1.1\ \mu\Omega$ cm. The decrease in the temperature-independent contribution to the resistivity when going from high to low temperatures comes from a gradual reduction in the spin-disorder scattering due to lifting the degeneracy of the $^2F_{5/2}$ multiplet.[18] Concurrently, the Kondo effect observed at high temperatures refers to the entire multiplet while that in the LT interval is associated with the crystal-field ground state. According to Ref. 18, the ratio of the logarithmic slopes in $\rho(T)$ is governed only by the effective degeneracies λ_i of the crystal-field levels involved in the Kondo effect, i.e.,

$$\frac{c_{\mathrm{K,LT}}}{c_{\mathrm{K,HT}}}=\frac{\lambda_L^2 T-1}{\lambda_H^2 T-1}. \tag{2}$$

In the case of $CeRh_2Si$ the ratio of the Kondo coefficients is roughly 3:33 being in very good agreement with the theoretical prediction for the ground doublet—entire $^2F_{5/2}$ multiplet scenario (3:35).

As displayed in the inset of Fig. 2, the temperature derivative of the resistivity of $CeRh_2Si$ exhibits a distinct feature below 2 K that is related to the onset of magnetically ordered state (cf. the heat-capacity results discussed below). The nonphononic resistivity in the ordered region can be well described by the function $\Delta\rho(T)=\rho_0+AT^2$ with the parameters $\rho_0=21.9\ \mu\Omega$ cm and $A=18.8\ \mu\Omega\ \mathrm{cm/K^2}$. The first term in this formula accounts for scattering processes of conduction electrons on static defects, i.e., ρ_0 is the residual resistivity, whereas the second term has a form characteristic of Fermi liquids and/or isotropic ferromagnets.

Upon applying magnetic field perpendicular to the electrical current, the resistivity hardly changes above 15 K but in the low-temperature region a pronounced magnetogalvanic effect occurs. As may be inferred from Fig. 3, the resistivity measured in 9 T lacks the low-temperature logarithmic upturn, and the kink due to the magnetic phase transition is smeared out and shifted to higher temperatures. The magnetoresistance defined as $\mathrm{MR}=\frac{\rho(H)-\rho(0)}{\rho(0)}$ is negative except for the region below 0.6 K. The influence of the magnetic field on the resistivity is shown in more detail in Fig. 4. In fields lower than 3 T, $\rho(T)$ does not change significantly, and the inflection point associated with the onset of the ordered state slightly shifts toward lower temperatures, as usually observed for antiferromagnets. In stronger fields, more distinct changes in $\rho(T)$ are seen. In particular, together with gradual suppression of the resistivity there occurs a systematic shift of the magnetic phase transition toward higher temperatures, in a manner known for ferromagnetic systems.

Another important feature is a continuous increase with increasing the magnetic field strength of the low-temperature interval in which the electrical resistivity gets strongly suppressed. The latter effect my be better inferred from Fig. 5 that displays the transverse magnetoresistance probed in magnetic fields ranging from 0.5 to 9 T. The magnetoresistance is negative from about 20 K in each field down to a temperature of 1.5 K in a field of 0.5 T and to 0.6 K in 9 T. Close to the magnetic phase transition, a minimum in MR(T) forms. It is relatively shallow for $\mu_0 H \leq 1$ T but rapidly becomes very deep in stronger fields. In 9 T, the magnitude of MR at its minimum is as large as −56%. On the MR isotherm measured in 0.5 T one recognizes a weak local maximum in the positive magnetoresistance that is often observed for antiferromagnets. This maximum gets shifted to lower temperature in a field of 1 T and entirely disappears in stronger fields. All these observed features clearly manifest a substantial field-induced change in the character of the magnetic state. They are consistent with the scenario of antiferromag-

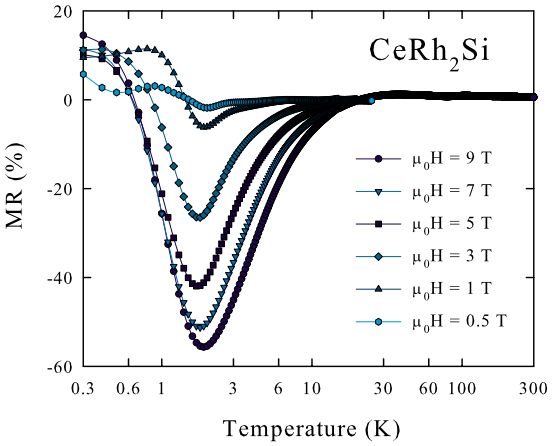

FIG. 5. (Color online) Temperature variation in the transverse magnetoresistance of $CeRh_2Si$ measured in several different magnetic fields. Note the logarithmic temperature scale.

netic ordering in zero-field and metamagnetic transformation to field-induced ferromagnetism above 1 T (see below). In fields $\mu_0 H \geq 3$ T, the positive magnetoresistance found at the lowest temperatures appears nearly field independent and equal to about 11%. Such positive contribution to MR can be expected for Kondo lattices in their coherent scattering regime.

Figure 6(a) displays the transverse magnetoresistance measured as a function of the magnetic field strength at several different temperatures from the paramagnetic range. At each temperature MR is negative. The isotherm taken at 4.4 K has largely a convex shape yet slightly bends upwards in high magnetic fields to reach −33% in 8 T. In turn, the MR(H) curves measured at higher temperatures have a convex character in the entire field range studied, and with increasing field the MR value in $\mu_0 H = 8$ T gradually decreases.

The overall character of the MR(H) isotherms of $CeRh_2Si$ is reminiscent to that characteristic of Kondo compounds[19] but it is also compatible with the behavior predicted for ferromagnets above their ordering temperature.[20] For both classes of materials MR is expected to scale as MR $= f[H/(T+T^*)]$, where the parameter T^* is related to their characteristic temperatures (either Kondo or Curie), namely, $T^* \simeq T_K$ and $T^* \simeq -T_C$, respectively.

In order to test this scaling relation, the magnetoresistivity data of $CeRh_2Si$ were replotted as a function of $H/(T+T^*)$, where the characteristic temperature T^* was adjusted so to achieve the best overlap of the MR curves measured for $6 \leq T \leq 20$ K. The 4.3 K isotherm was excluded from the analysis because of its dissimilar overall shape, likely manifesting short-range magnetic exchange interactions. In turn, the MR data obtained at higher temperatures were not taken into account because of possible contributions due to excited crystal-field states. As displayed in Fig. 6(b), the MR isotherms measured at different temperatures can be superimposed on a single curve if $T^* = -2$ K is assumed (reducing or increasing T^* by 0.5 K made the overlap between particular MR curves noticeably worse). The negative sign of T^* implies that the observed scaling should be attributed to the

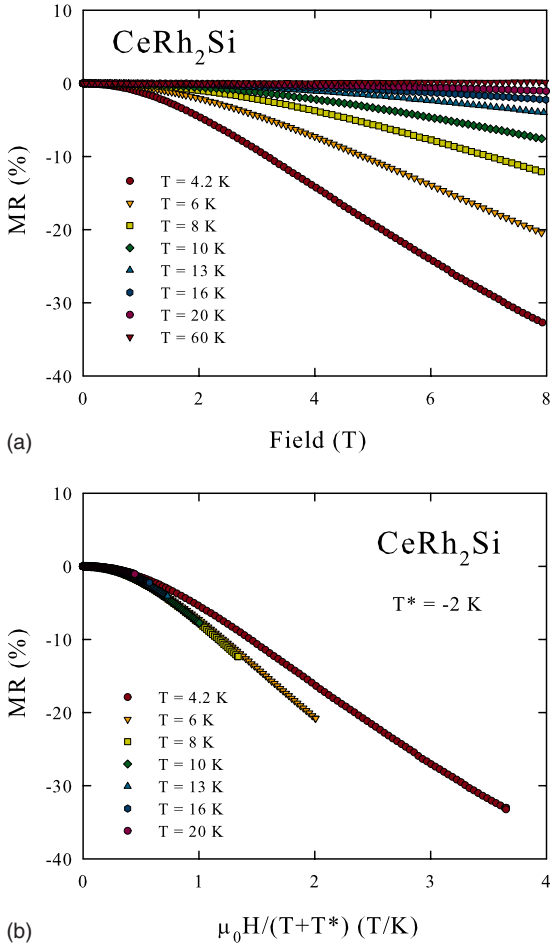

FIG. 6. (Color online) (a) Magnetic field dependencies of the transverse magnetoresistance of $CeRh_2Si$ taken at several temperatures in the paramagnetic state. (b) Schlottmann scaling of the magnetoresistance data of $CeRh_2Si$.

ferromagnetic character of magnetic correlations in the compound studied. Most significantly, the value of $|T^*|$ is very close to the temperature of the magnetic phase transition observed in the electrical resistivity and heat-capacity data. On the contrary, its absolute value is distinctly different from the Kondo temperature in $CeRh_2Si$, which was estimated from the magnetic susceptibility data to be about 16 K.

3. Heat capacity

Figure 7(a) displays the low-temperature behavior of the specific heat of $CeRh_2Si$. Pronounced λ-shaped anomaly in $C(T)$ unambiguously manifests the magnetic phase transition that occurs at 1.65(5) K. The specific-heat jump at the onset of the ordered state is much smaller than that expected for a doublet ground state within the molecular-field approximation [$\Delta C = 12.47$ J/(mol K^2)], and this reduction most likely arises due to the Kondo effect. Another small feature in $C(T)$ is seen near 4.5 K. This singularity occurs due to the aforementioned contamination of the sample studied by small amount of $CeRh_3Si_2$.[13] As displayed in the inset of Fig. 7(a), above 10 K, the specific-heat data can be described by the standard formula $C(T) = \gamma T + \beta T^3$, where the two terms ac-

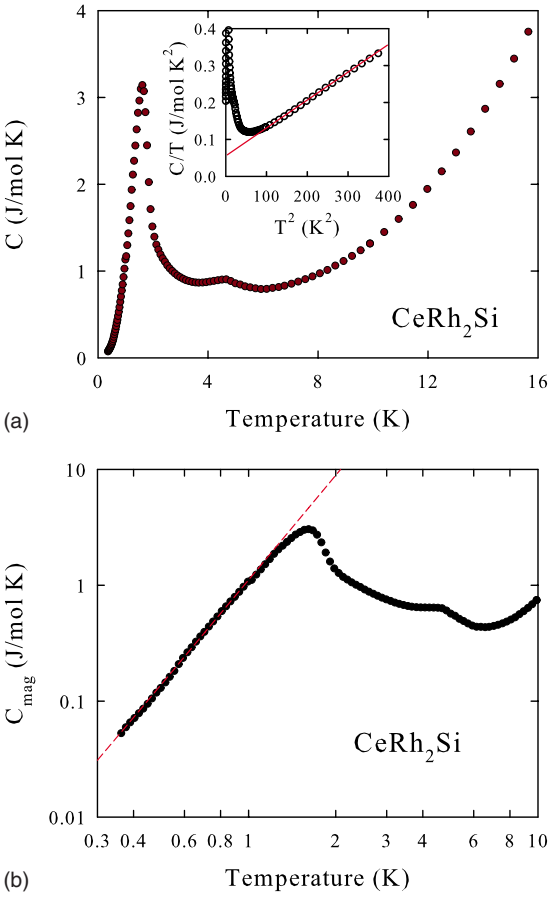

FIG. 7. (Color online) (a) Low-temperature dependence of the specific heat of $CeRh_2Si$. Inset: the specific-heat data in the form C/T versus T^2 [for the sake of clarity the vertical scale was cut at a value of 0.4 J/(mol K^2)]. The solid line is a linear fit discussed in the text. (b) Analysis of the magnetic contribution to the specific heat of $CeRh_2Si$ (see the text). Note double-logarithmic scale.

count for the electronic and phonon contributions, respectively. The least-squares fit yields a moderately enhanced Sommerfeld coefficient $\gamma=58$ mJ/(mol K^2) that is about half the value reported for $CeRh_2Si$ in Ref. 15. In turn, from the relation $\beta=\frac{12\pi^4}{5}\frac{nR}{\Theta_D^3}$ (r stands for a number of atoms in the formula unit and R is the universal gas constant) one calculates the Debye temperature $\Theta_D=236$ K, in good agreement with the value of 250 K reported before.[15]

The magnetic contribution to the specific heat of $CeRh_2Si$ can be derived by subtracting from the measured data the electronic and phonon terms. Taking into account the above derived values of γ and β one obtains the magnetic specific heat $C_{mag}(T)=C(T)-\gamma T-\beta T^3$, displayed in Fig. 7(b). The double-logarithmic scale, used in this figure, clearly reveals a power-law temperature variation in C_{mag} in the magnetically ordered state. Quantitatively, the experimental data up to 1.2 K can be approximated by the formula $C_{mag}(T)=c_{SW}T^3$ with the coefficient $c_{SW}=1.11$ J/(mol K^4). The observed T^3 power-law dependence of the specific heat points to an antiferromagnetic character of the ordered state. Another indication for the ground-state antiferromagnetism in $CeRh_2Si$ can be inferred from the heat-capacity data taken in applied magnetic fields. As shown in Fig. 8, with increasing the magnetic field strength up to 1 T, the peak in $C/T(T)$ gradually shifts to lower temperatures, while this variation gets reversed for $\mu_0 H \geq 3$ T. At the same time, the maximum in $C(T)$ becomes very broad in strong fields. Such a behavior is characteristic of antiferromagnets that exhibit magnetic field induced metamagnetic phase transitions. For $CeRh_2Si$ the metamagnetic critical field is likely between 1 and 3 T.

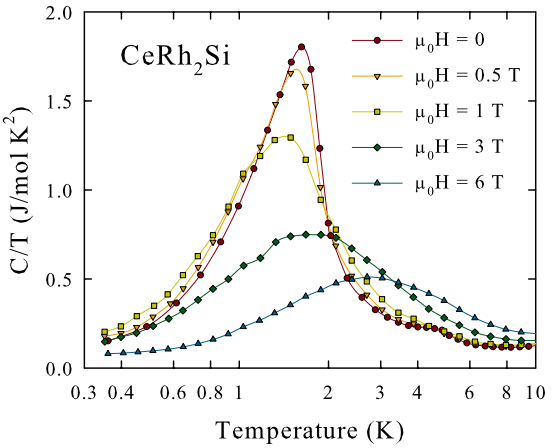

FIG. 8. (Color online) Temperature variation in the specific heat over temperature ratio of $CeRh_2Si$ measured in several different external magnetic fields. Note the logarithmic temperature scale.

The temperature dependence of the entropy in $CeRh_2Si$ is shown in Fig. 9. At the magnetic phase transition, the entropy is strongly reduced in comparison to the entropy of the ground-state doublet and amounts only to about $0.29R\ln 2$ (the value of $R\ln 2$ is achieved at a temperature as high as ≈ 20 K). This feature is in concert with the reduced value of the jump ΔC at the critical temperature, and together with the enhanced value of γ supports the Kondo effect scenario, inferred from the electrical transport behavior of the compound. According to Desgranges and Schotte,[21] the entropy of a Kondo system amounts to $0.68R\ln 2=3.92$ J/(mol K) at the characteristic temperature T_K. This relation yields for

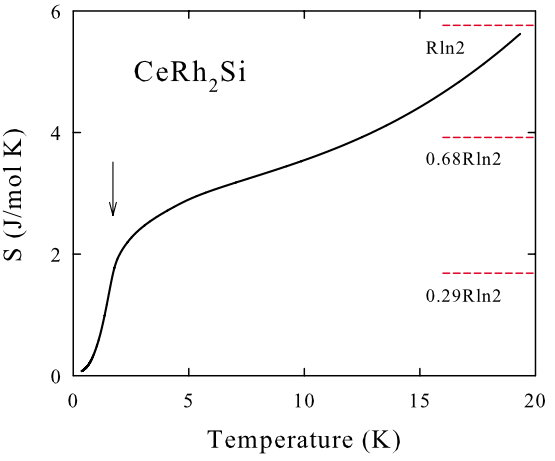

FIG. 9. (Color online) Temperature variation in the entropy in $CeRh_2Si$. The arrow marks the magnetic phase transition observed in the specific-heat data.

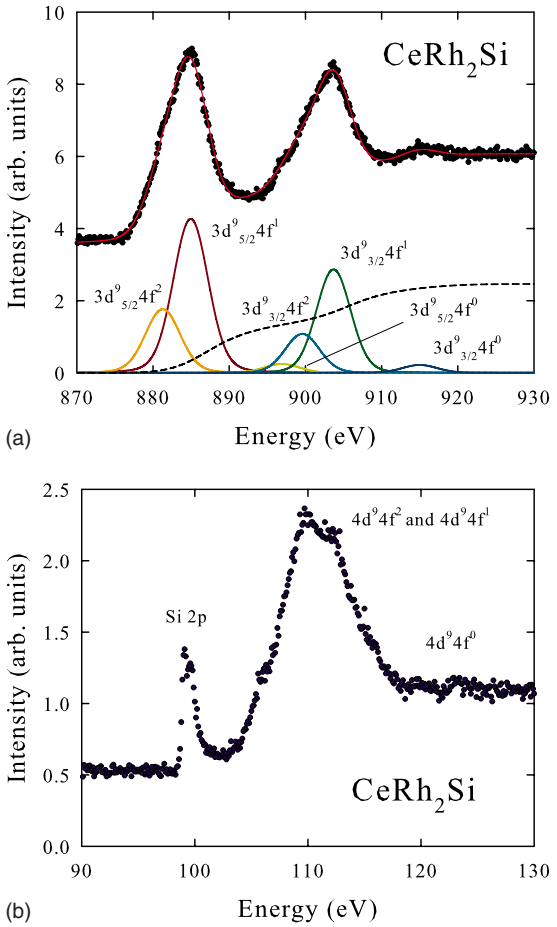

FIG. 10. (Color online) (a) Ce $3d$ XPS spectrum of $CeRh_2Si$. Background was calculated using the Tougaard algorithm (Ref. 22) and subtracted from the measured XPS data. The f^0, f^1, and f^2 components were separated as described in the text. (b) Ce $4d$ XPS spectrum of $CeRh_2Si$.

$CeRh_2Si$ the Kondo temperature of about 12.5 K, in fairly good agreement with the value estimated from the magnetic susceptibility data.

B. Electronic structure

The $3d$-core-level XPS spectrum measured for $CeRh_2Si$ is shown in Fig. 10(a). Due to the spin-orbit (SO) interaction, it consists of two sets of photoemission lines, split by $\Delta_{SO}=18.6$ eV, which should be assigned to the $3d_{3/2}$ and $3d_{5/2}$ components of the final states. Each SO set may contain three contributions, which correspond to the possible f^0, f^1, and f^2 configurations of the Ce ion.[23,24] Their separation can be done based on the Doniach-Šunjić theory,[25] and the result of such deconvolution for the compound studied is presented in the bottom of Fig. 10(a). The main peaks $3d^9f^1$ originate from trivalent Ce ions while weak structures located about 11 eV away from the main peaks are due to the $3d^9f^0$ component and hint at somewhat unstable character of the $4f$ shell. In turn, the $3d^9f^2$ final-state components are located on the low-energy side of the main lines at the distance of about 4 eV. They appears when the core hole becomes screened by an additional $4f$ electron due to the hybridization of the Ce $4f$ shell with the conduction band. Consequently, from their contribution to the measured Ce $3d$ spectrum one can derive the hybridization energy $\Delta=\pi V^2N(\epsilon_F)$, which describes the hybridization part of the Anderson impurity Hamiltonian [V is the hybridization matrix element and $N(\epsilon_F)$ is the density of states at the Fermi energy E_F].[26]

Quantitative analysis of the $3d$ spectrum of $CeRh_2Si$ was performed based on the approach developed by Gunnarsson and Schönhammer[27] (for details on the method applied see Refs. 24 and 28). The ratio $I(f^2)/[I(f^1)+I(f^2)]$ of the intensities of the particular components to the spectrum yields $\Delta\approx 140$ meV while from the ratio $I(f^0)/[I(f^0)+I(f^1)+I(f^2)]$ the mean occupation of the $4f$ level is estimated to be $n_f\geq 0.95$. The obtained values of Δ and n_f imply some valence instability of the cerium ions and hence provide another evidence for the Kondo lattice character of the compound studied. Assuming that in $CeRh_2Si$ the density of states at E_F is of similar magnitude as that calculated for a few other phases from the Ce-Rh-Si system, i.e., $N(\epsilon_F)\geq 1$ state per electron volt per atom,[10,12,13] one gets an estimate for the hybridization matrix element $V<100$ meV. Such value is typical for heavy-fermion materials in which heavy masses are associated with the on-site hybridization between the $4f^1$ states of Ce^{3+} ions and the conduction-band states. Due to this interaction the $4f$ electrons become partially delocalized, which manifests itself in the fractional valence of cerium, that is slightly larger that +3, just as observed for $CeRh_2Si$.

Figure 10(b) presents the Ce $4d$ XPS spectrum of $CeRh_2Si$. It consists of relatively broad features located at binding energies from 103 to 118 eV and hardly resolved structure in the energy region 118–124 eV. Moreover, there occurs a sharp peak near 100 eV. Whereas the latter feature likely arises due to $2p$ band of silicon, the main peaks should be attributed to two sets of photoemission lines associated with the $4d^94f^1$ and $4d^94f^2$ final states. The observed splitting $\delta=3.1$ eV is close the value expected for the SO splitting of the La $4d$ states and thus corresponds to the core hole $4d$ spin-orbit interaction. Similar splitting may be inferred for the weak peaks at higher binding energies, and hence these features should consequently be assigned to the $4d^94f^0$ final states. Their appearance provides another evidence for slightly delocalized character of the $4f$ electrons in the compound studied.[24,29,30] As characteristic for cerium intermetallics,[30] strong exchange interaction between the $4d$ and $4f$ electrons results in the formation of complicated multiplet structure, and therefore more detailed interpretation of the Ce $4d$ XPS spectrum of $CeRh_2Si$ seems not possible.

IV. SUMMARY

The compound $CeRh_2Si$ crystallizes with an orthorhombic unit cell[14] that is a site exchange variant of the well-known $CeNiSi_2$-type structure. At variance with the literature data,[15] which claimed the spin-glass behavior below the freezing temperature of 1 K, the studied polycrystalline sample was found to exhibit a long-range magnetic ordering below 1.65 K. Though no direct proof of the character of the

electronic ground state via magnetic measurements was possible in the present study (because of the limited temperature range), the observed magnetic field-induced changes in the temperature variations in the specific heat and the electrical resistivity suggest an antiferromagnetic arrangement of the magnetic moments. Nevertheless, the presence of dominant ferromagnetic correlations was inferred from the magnetoresistance data taken in the paramagnetic state in strong magnetic fields. In line with this finding seems rather small value of the critical field leading to a metamagnetic phase transition. To account for simultaneous observation of ferromagnetic and antiferromagnetic exchange interactions one may speculate that the layered pseudotetragonal and strongly elongated ($b > 4a \approx 4c$) crystal structure of $CeRh_2Si$ may promote the formation of strongly ferromagnetically coupled layers of Ce atoms, which alternate in an antiferromagnetic manner along the long crystallographic axis, hence yielding the antiferromagnetic unit cell. Obviously, this presumed magnetic structure requires verification by neutron diffraction.

Alike established before for several other intermetallics from the ternary Ce-Rh-Si system,[2,5,11] the low-temperature physical properties of $CeRh_2Si$ are influenced by strong Kondo screening interactions. The electrical resistivity and the specific-heat data reveal a Kondo lattice character of the compound studied with the characteristic temperature of 12–16 K. Hybridization of the cerium 4*f* states with the conduction band governs the electronic structure near the Fermi level and manifests itself in the 3*d* and 4*d* core level XPS spectra. The large hybridization energy of about 140 eV and significantly reduced mean occupancy of the 4*f* level of about 0.95, derived from this data, imply instability of the cerium valence state. Further spectroscopic studies are necessary to provide more information on the electronic structure of the compound.

ACKNOWLEDGMENTS

The authors are grateful to Agnieszka Kondrat for her involvement into this study at its initial stage. The work was supported by the Ministry of Science and Higher Education within the research Projects No. N202 116 32/3270 and No. NN202 032137.

[1] E. Bauer, G. Hilscher, H. Michor, C. Paul, E. W. Scheidt, A. Gribanov, Y. Seropegin, H. Noël, M. Sigrist, and P. Rogl, Phys. Rev. Lett. **92**, 027003 (2004).
[2] N. Kimura, K. Ito, K. Saitoh, Y. Umeda, H. Aoki, and T. Terashima, Phys. Rev. Lett. **95**, 247004 (2005).
[3] I. Sugitani, Y. Okuda, H. Shishido, T. Yamada, A. Thamizhavel, E. Yamamoto, T. D. Matsuda, Y. Haga, T. Takeuchi, R. Settai, and Y. Onuki, J. Phys. Soc. Jpn. **75**, 043703 (2006).
[4] A. Lipatov, A. Gribanov, A. Grytsiv, S. Safronov, P. Rogl, J. Rousnyak, Y. Seropegin, and G. Giester, J. Solid State Chem. **183**, 829 (2010).
[5] R. Settai, A. Misawa, S. Araki, M. Kosaki, K. Sugiyama, T. Takeuchi, K. Kindo, Y. Haga, E. Yamamoto, and Y. Onuki, J. Phys. Soc. Jpn. **66**, 2260 (1997).
[6] R. Movshovich, T. Graf, D. Mandrus, J. D. Thompson, J. L. Smith, and Z. Fisk, Phys. Rev. B **53**, 8241 (1996).
[7] Y. Ōnuki, R. Settai, K. Sugiyama, T. Takeuchi, T. C. Kobayashi, Y. Haga, and E. Yamamoto, J. Phys. Soc. Jpn. **73**, 769 (2004).
[8] T. Akazawa, H. Hidaka, H. Kotegawa, T. C. Kobayashi, T. Fujiwara, E. Yamamoto, Y. Haga, R. Settai, and Y. Onuki, J. Phys. Soc. Jpn. **73**, 3129 (2004).
[9] P. W. Anderson, Phys. Rev. B **30**, 4000 (1984).
[10] D. Kaczorowski, A. P. Pikul, U. Burkhardt, M. Schmidt, A. Ślebarski, A. Szajek, M. Werwiński, and Y. Grin, J. Phys.: Condens. Matter **22**, 215601 (2010).
[11] M. Szlawska, D. Kaczorowski, A. Ślebarski, L. Gulay, and J. Stępień-Damm, Phys. Rev. B **79**, 134435 (2009).
[12] D. Kaczorowski, Y. Prots, U. Burkhardt, and Y. Grin, Intermetallics **15**, 225 (2007).
[13] A. P. Pikul, D. Kaczorowski, Z. Gajek, J. Stępień-Damm, A. Ślebarski, M. Werwiński, and A. Szajek, Phys. Rev. B **81**, 174408 (2010); A. P. Pikul and D. Kaczorowski, Acta Phys. Pol. A **115**, 235 (2009); D. Kaczorowski and T. Komatsubara, Physica B **403**, 1362 (2008).
[14] A. I. Tursina, A. V. Gribanov, Y. D. Seropegin, A. A. Novitskii, and O. I. Bodak, J. Alloys Compd. **367**, 146 (2004).
[15] Y. Muro, S. Takahashi, K. Sunahara, K. Motoya, M. Akatsu, and N. Shirakawa, J. Magn. Magn. Mater. **310**, e40 (2007).
[16] O. I. Bodak and E. I. Gladyshevskii, Kristallografiya **14**, 990 (1969) [Sov. Phys. Crystallogr. **14**, 859 (1970)].
[17] A. C. Hewson, *The Kondo Problem to Heavy Fermions* (Cambridge University Press, Cambridge, England, 1993).
[18] D. Cornut and B. Coqblin, Phys. Rev. B **5**, 4541 (1972).
[19] B. Andraka and G. R. Stewart, Phys. Rev. B **49**, 12359 (1994); B. Andraka, *ibid.* **52**, 16031 (1995).
[20] J. H. Cho, Q. X. Jia, X. D. Wu, S. R. Foltyn, and M. P. Maley, Phys. Rev. B **54**, 37 (1996).
[21] H.-U. Desgranges and K. D. Schotte, Phys. Lett. **91A**, 240 (1982).
[22] S. Tougaard and P. Sigmund, Phys. Rev. B **25**, 4452 (1982).
[23] G. Crecelius, G. K. Wertheim, and D. N. E. Buchanan, Phys. Rev. B **18**, 6519 (1978).
[24] J. C. Fuggle, F. U. Hillebrecht, Z. Żołnierek, R. Lässer, C. Freiburg, O. Gunnarsson, and K. Schönhammer, Phys. Rev. B **27**, 7330 (1983).
[25] S. Doniach and M. Šunjić, J. Phys. C **3**, 285 (1970).
[26] P. W. Anderson, Phys. Rev. **124**, 41 (1961).
[27] O. Gunnarsson and K. Schönhammer, Phys. Rev. B **28**, 4315 (1983).
[28] A. Ślebarski, T. Zawada, J. Spałek, and A. Jezierski, Phys. Rev. B **70**, 235112 (2004).
[29] A. J. Signorelli and R. G. Hayes, Phys. Rev. B **8**, 81 (1973).
[30] Y. Baer, R. Hauger, Ch. Zürcher, M. Campagna, and G. K. Wertheim, Phys. Rev. B **18**, 4433 (1978).